

## Tunable visual color filter using microfluidic grating

Z. G. Li,<sup>1,2</sup> Y. Yang,<sup>1</sup> X. M. Zhang,<sup>3,a)</sup> A. Q. Liu,<sup>1</sup> J. B. Zhang,<sup>2</sup> L. Cheng,<sup>4</sup>  
and Z. H. Li<sup>5</sup>

<sup>1</sup>*School of Electrical and Electronic Engineering, Nanyang Technological University, Nanyang Avenue, Singapore 639798, Singapore*

<sup>2</sup>*Data Storage Institute, 5 Engineering Drive 1, Singapore 117608, Singapore*

<sup>3</sup>*Department of Applied Physics, Hong Kong Polytechnic University, Kowloon, Hong Kong*

<sup>4</sup>*Department of Mechanical Engineering, Faculty of Engineering, National University of Singapore, 21 Lower Kent Ridge Road, Singapore 119077, Singapore*

<sup>5</sup>*State Key Laboratory of Nonlinear Mechanics, Institute of Mechanics, Chinese Academy of Sciences, 15 Beisihuanxi Road, Beijing 100080, China*

(Received 10 August 2010; accepted 30 August 2010; published online 30 December 2010)

This paper reports a tunable visual color filter based on a microfluidic transmission grating. The grating lines are formed by the microflows in an array of evenly spaced straight microchannels. In experimental study, the transmission of white light measures a shift of visual color from red to blue in the zeroth order diffraction in response to a change of the refractive index from 1.3290 to 1.3782 in the microflows. The merit of large tunability of transmission peak ( $\Delta\lambda=408$  nm) makes this grating potential for various applications in biological and chemical measurements, such as space- and time-resolving micropattern spectrophotometers and separation of the fluorescence from the excitation. © 2010 American Institute of Physics. [doi:10.1063/1.3491469]

### I. INTRODUCTION

Visual color filters have wide applications in display, image sensors, spectrometers, and fluorescence detections.<sup>1</sup> The conventional color filters mostly utilize spin cast dye films to transmit the desired wavelength range while absorbing the others, which places a fundamental limit to the transmission efficiency ( $<1/3$ ) and causes significant heat problems due to the absorption. Recently grating has become an alternative technology to construct the visual color filters due to its capabilities of miniaturization and design flexibility. Most of the demonstrated researches employ solid materials (such as aluminum, polysilicon, and rigid polymers) or liquid crystals to form the desired groove profiles of the gratings.<sup>1-5</sup> Although outstanding optical performance has been achieved, the use of solid materials severely limits the tunability of parameters, such as refractive index contrast and spectrum range, and thus increases the complexity of the optical systems that require large tuning ranges. Therefore, a number of gratings have to be used to produce primary colors, which are then superimposed to produce full color scheme.<sup>4,5</sup> The systems thus become really complicated.

On the other hand, optofluidics has recently emerged as an exciting research field of applied science and technology with broad applications in chemistry and biomedical engineering.<sup>6-11</sup> By combining the microfluidic and optical components into a single miniaturized platform, optofluidics provides a simple way to integrate optical sensing functionalities into laboratory-on-a-chip systems and has inspired the creation of many new types of optofluidic elements, such as liquid-liquid waveguides,<sup>12,13</sup> optofluidic lenses,<sup>14,15</sup> switches,<sup>16</sup> lasers,<sup>17</sup> and microscopes.<sup>18</sup> Similarly,

<sup>a)</sup> Author to whom correspondence should be addressed. Electronic mail: apzhang@inet.polyu.edu.hk.

optofluidics could offer new platforms to construct the widely tunable gratings for the color filters due to its unique ability to change the fluid properties over a large range (for example, by simply replacing one fluid with another).

By such foresight, optofluidic gratings have recently attracted increasing interests of research. A prominent work is the tunable diffraction grating employing a flowing lattice of bubbles.<sup>19</sup> The two-dimensional (2D) bubble lattice on a microfluidic platform is formed by the self-assembly of bubbles injected from a flow-focusing bubble generator. The 2D grating can be tuned by changing the pressures and the rates of flow applied to the devices. In another study,<sup>20</sup> droplets have been demonstrated to form long period grating structures by alternating short sections of two immiscible solutions (e.g.,  $\text{CaCl}_2$  solution and oil). It follows the same principle as the long period fiber grating but the grating property is tuned by adjusting the flow rate or the fluid's refractive index. Compared with the 2D and long period gratings, one-dimensional grating has actually much wider application in almost every aspect of optics and photonics. However, its optofluidic implementation has yet to attract due attentions. This paper will present a tunable optofluidic transmission phase grating and will demonstrate its functionality as the zeroth order visual color filter. The grating consists of an array of evenly spaced straight microchannels. Each grating line is formed by a flowing stream in a microchannel. The tunability of the grating diffraction pattern can be achieved by dynamic modulation of the refractive index of all the microflows at the same time.

## II. DEVICE DESIGN AND ANALYSIS

The measurement setup and the cross-sectional view of the optofluidic transmission phase grating are shown in Figs. 1(a) and 1(b). The grating consists of two regions with different refractive indices. One region is the solid polymer structure with a refractive index  $n_0$  and the other is the microflows within the microchannel array with a refractive index  $n_1$ . The phase difference  $\xi$  between the solid polymer region and the microflow region can be expressed as<sup>21</sup>

$$\xi = 2\pi t(n_0 - n_1)/\lambda, \quad (1)$$

where  $t$  is the thickness of the grating structure,  $\lambda$  is the wavelength of the incident beam, and  $(n_0 - n_1)$  is the refractive index contrast of the two regions. It is easy to see from Eq. (1) that the phase difference can be varied by changing  $t$ ,  $\lambda$ , or  $n_1$ . In optofluidic chips, it is often more convenient to modulate  $n_1$  than to change  $t$ . By whichever method, the change of  $\xi$  would modify the intensity of the zeroth diffraction order following the relationship as<sup>21,22</sup>

$$I_{m=0} = I_0 \cos^2(\xi/2), \quad (2)$$

where  $m$  is the order number of the diffraction pattern and  $I_0$  is the incident intensity. For a single wavelength incident light, if  $\xi$  is increased within one period from 0 to  $\pi$ , the diffraction intensity of the zeroth order for the specific wavelength  $\lambda$  is decreased from maximum to 0. For a broadband incident light, such as the white light which contains many wavelength components, the zeroth diffraction order would exhibit certain color pattern for whatever the values of  $t$  and  $n_1$ . Some wavelength satisfies  $\xi = 2m\pi$  ( $m$  is integer) and enjoys maximum transmission while the others are partially transmitted or even blocked. As different wavelength components are spatially overlapped in the zeroth order, they all contribute to the perception of color, resulting in a specific visual color. With the change of  $n_1$ , the zeroth diffraction order would experience a variation of the visual color.

For theoretical analysis, a MATLAB code is developed for predicting the grating diffractions. The incident light is assumed to be a broadband light source with a uniform spectral distribution in the visible range. The grating parameters used in simulation are chosen identical to those of the fabricated grating sample to be used in the experimental study. Here the grating period  $\Lambda$  is 20  $\mu\text{m}$ , the fill factor  $f$  is 50%, and the grating thickness  $t$  is 29.5  $\mu\text{m}$ . The value of  $n_0$  is assumed to be 1.4168, which is the refractive index of polydimethylsiloxane (PDMS) material. The calculated spectra of the zeroth order diffraction over the wavelength range of 300–900 nm are shown in Fig. 2(a) for six liquid samples with the refractive indices  $n_a = 1.3290$ ,  $n_b = 1.3436$ ,  $n_c = 1.3567$ ,

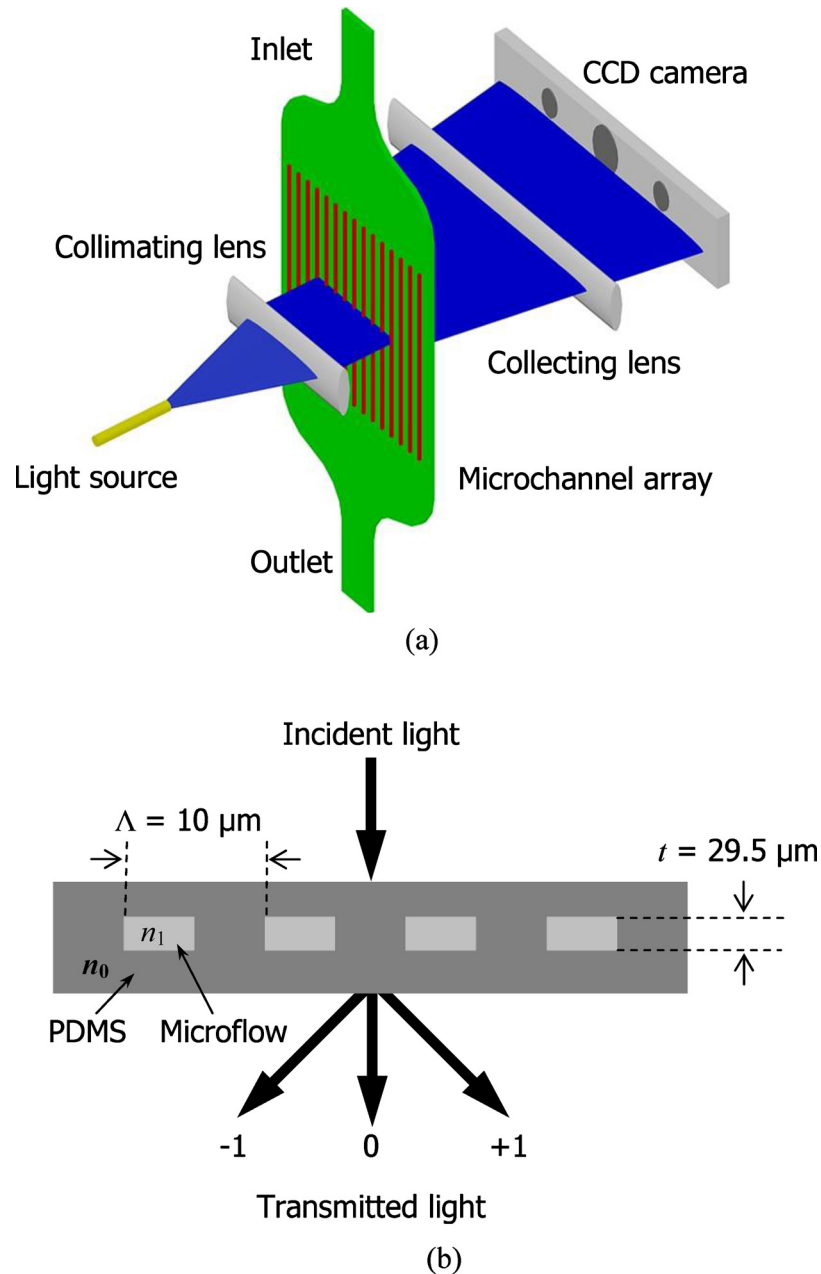


FIG. 1. (a) Schematic of the experimental setup of the tunable transmission phase grating; (b) the cross-sectional view of the grating and the diffraction orders of the transmission (not to scale).

$n_d=1.3715$ ,  $n_e=1.3770$ , and  $n_f=1.3782$ , respectively. Here the wavelength range is chosen intentionally to be larger than the typical visible range of 380–750 nm so as to reflect the filtering properties at the two ends of visible range. It can be observed that the peak wavelength is shifted from 727 nm to 614, 497, 375, 329, and then 319 nm in response to the change of refractive index from  $n_d$  to  $n_f$ . As explained above, the change of peak wavelength would cause a prominent change of the visual color in the zeroth order diffraction.

### III. FABRICATION AND EXPERIMENTAL RESULTS

In fabrication, an optofluidic transmission phase grating is obtained by standard soft-lithography technology using PDMS material. The mold is fabricated using an SU-8 master. After

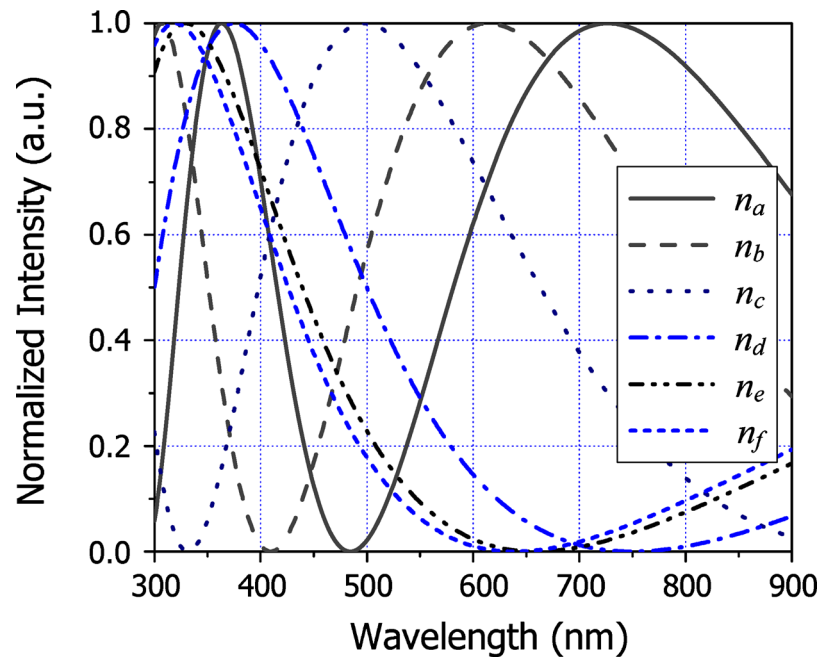


FIG. 2. Theoretical results of the zeroth diffraction order transmission spectra in the visible range in response to the modulation of the refractive index of the microflows. The values of refractive indices  $n_a$  to  $n_f$  correspond to 1.3290, 1.3436, 1.3567, 1.3715, 1.3770, and 1.3782, respectively.

the PDMS layer is peeled off from the mold, the inlets and outlets are manually punched. Finally, the PDMS layer with rectangular grooves is bonded onto another PDMS substrate using oxygen-plasma surface treatment method. A micrograph of the grating structure is shown in Fig. 3(a). To enhance the picture visibility, the fluid is colored with dark green dye to differentiate the solid PDMS region and the microflow region. However no dye is applied in the following experiment.

In the experimental study, the transmission diffractions of a white light source are measured to examine the performance of the fabricated grating sample. The experimental setup follows the diagram in Fig. 1(a). It consists of a halogen light source (HL-2000-FHSA, Ocean Optics), a collimating lens, the optofluidic grating sample, a collecting lens, and a charge coupled device camera (CCD). The incident white light from a single-mode optical fiber is first collimated by the collimating lens (double convex,  $f=20$  mm, diameter of 20 mm) before being projected onto the liquid/solid grating region. Then the diffraction patterns are focused by the collecting lens and are finally recorded by the CCD camera (DS-70, Olympus, exposure time 1/100 s). For the convenience of experimental observation, the collecting lens utilizes actually an inverted system optical microscope (TS 100 Eclipse, Nikon, with a 20 $\times$  objective lens). For the measurement of the transmission spectrum, the CCD camera is replaced by a spectrometer (HR4000, Ocean Optics, 200–1100 nm). Six ethylene glycol monomethyl ether solutions are injected into the microchannel array by syringe pumps (NE-1000, New Era). The refractive indices of the solutions are the same as those used in the simulation. Figure 3(b) exemplifies the observed diffraction patterns of the zeroth and first orders under the microscope when the refractive index of the solution is 1.3567. It can be seen that the two diffraction orders are well separated. The zeroth order is a circular spot while the first order exhibits a rainbowlike pattern over an angle range of 1.6 $^\circ$ –3.4 $^\circ$ . In the first order, there is a dark line in the yellow color range, which corresponds to the peak transmission of the zeroth order. The diffraction angle of the dark line is 2.3 $^\circ$ .

The diffraction patterns of the zeroth order for the six solutions are shown in Fig. 3(c). From  $n_a$  to  $n_f$ , the visual color varies from red, orange, yellow, green, cyan to finally blue. The observed change of visual colors is a clear manifestation of the color filtering effect. Based on the CIE 1931 standard, colors produced in the zeroth order of the optofluidic grating are plotted in the CIE xyY

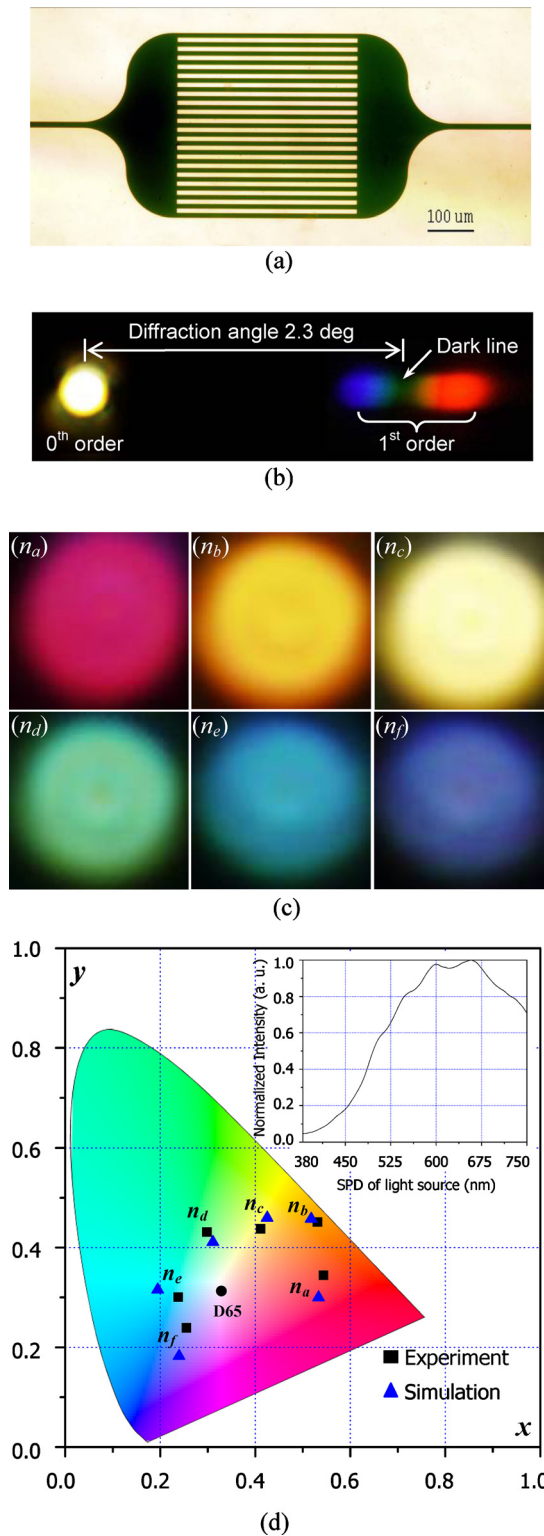


FIG. 3. Experimental results. (a) Micrograph of the fabricated device of optofluidic transmission phase grating, the fluid is colored to enhance the visibility of pictures; (b) observed diffraction patterns of the zeroth and first orders in the case of  $n_c=1.3567$ ; (c) measured diffraction patterns of the zeroth diffraction order that exhibit different visual colors. The values of refractive indices  $n_a$  to  $n_f$  are the same as those in Fig. 2; (d) chromaticity values of the visual colors produced in the zeroth diffraction order by the optofluidic transmission phase grating. The inset shows the spectral power distribution of the light source.

color chart, as shown in Fig. 3(d). The chromaticity values  $x$  and  $y$  are calculated from the measured spectra. The point of D65 (6500 K) is chosen as the white point. It is seen that the measured points in the CIE chart are scattered around the white point. Particularly, those corresponding to  $n_a$  and  $n_b$  are quite far from the white point and produce close to monochromatic colors. However, those of  $n_3$  to  $n_6$  show less pure colors. One possible reason is that the intensities of the red (700 nm) and green (546 nm) band are too high as compared to that of the blue band (435.8 nm), as shown the inset of Fig. 3(d). This is why the visual color is tuned only from red to blue. If the light source has a uniform spectral density, the tuning range would cover the whole visible spectrum. For comparison, the CIE points for the simulation results are also presented in Fig. 3(d), which are calculated from Fig. 2 but with the consideration of the nonuniform spectral power distribution (SPD) of the light source [see the inset of Fig. 3(d)]. A rough match is obtained between the measurement and the simulation. The discrepancy mainly comes from the scattering of the microchannel edges and the roughness and dusts on the PDMS surface. However, the variation of visual color from red to blue has well proven that wide tuning can be obtained by reconfiguring the refractive index of the microflows.

#### IV. DISCUSSIONS

Such visual color filters could find particular applications in microfluidic based biochemical syntheses and measurements. For example, it can be used to separate the fluorescence light from the excitation light or separate different fluorescence lights.<sup>23</sup> Another possible application is the space- and time-resolving micropattern spectrophotometries, which utilize a transmission grating right on top of microfluidic samples to study the spectrum using a microscope.<sup>24</sup> Moreover, the color filter could be used to monitor the refractive index change of the microflows.<sup>25</sup> Based on the simulation results, a refractive index variation from 1.3290 to 1.3782 (i.e.,  $\Delta n \approx 0.05$ ) causes the peak wavelength to shift from 727 to 319 nm (i.e.,  $\Delta \lambda = 408$  nm). As a result, the sensitivity is  $8.3 \times 10^3$  nm/RIU, or equivalently  $1.2 \times 10^{-4}$  RIU/nm (here RIU stands for refractive index unit). The spectrometer used in the experiment has a resolution of 0.025 nm, therefore the minimum detectable change of refractive index is  $3.0 \times 10^{-6}$  RIU. With such a resolution over a range of about 0.05, the grating could be used to monitor the mixing effect in the micromixers,<sup>26</sup> the reaction kinetics of chemicals in microreactors,<sup>27</sup> the immobilization of DNA or proteins to the surface-treated microchannels, etc.

#### V. CONCLUSIONS

A visual color filter based on optofluidic solid/liquid transmission phase grating has been designed and experimentally demonstrated. The grating consists of a solid PDMS region and a microflow region, both of which are integrated onto a microfluidic chip. For white incident light, different visual colors in the zeroth order are obtained in response to the modulation of the refractive index of the microflows by simply changing the solution. Such color filter features a large tunability provided by the optofluidics and can be readily integrated with other microfluidic elements for laboratory-on-a-chip applications. It would find niche applications in biomedical and chemical measurements and analyses.

<sup>1</sup>D. K. Yang, *Inf. Disp.* **16**, 117 (2008).

<sup>2</sup>S. R. Kubota, *Opt. Photonics News* **13**, 50 (2002).

<sup>3</sup>B.-H. Cheong, O. N. Prudnikov, E. Cho, H.-S. Kim, J. Yu, Y.-S. Cho, H.-Y. Choi, and S. T. Shin, *Appl. Phys. Lett.* **94**, 213104 (2009).

<sup>4</sup>Y.-T. Yoon, H.-S. Lee, S.-S. Lee, S. H. Kim, J.-D. Park, and K.-D. Lee, *Opt. Express* **16**, 2374 (2008).

<sup>5</sup>K. Knop, *Opt. Commun.* **18**, 298 (1976).

<sup>6</sup>G. M. Whitesides, *Nature (London)* **442**, 368 (2006).

<sup>7</sup>G. H. W. Sanders and A. Manz, *Trends Analyt. Chem.* **19**, 364 (2000).

<sup>8</sup>T. M. Squires and S. R. Quake, *Rev. Mod. Phys.* **77**, 977 (2005).

<sup>9</sup>H. A. Stone, A. D. Strook, and A. Ajdari, *Annu. Rev. Fluid Mech.* **36**, 381 (2004).

<sup>10</sup>D. Psaltis, S. R. Quake, and C. Yang, *Nature (London)* **442**, 381 (2006).

<sup>11</sup>C. Monat, P. Domachuk, and B. J. Eggleton, *Nat. Photonics* **1**, 106 (2007).

<sup>12</sup>D. B. Wolfe, R. S. Conroy, P. Garstecki, B. T. Mayers, M. A. Fischbach, K. E. Paul, M. Prentiss, and G. M. Whitesides, *Proc. Natl. Acad. Sci. U.S.A.* **101**, 12434 (2004).

- <sup>13</sup>X. C. Li, J. Wu, A. Q. Liu, Z. G. Li, Y. C. Soew, H. J. Huang, K. Xu, and J. T. Lin, *Appl. Phys. Lett.* **93**, 193901 (2008).
- <sup>14</sup>S. K. Y. Tang, C. A. Stan, and G. M. Whitesides, *Lab Chip* **8**, 395 (2008).
- <sup>15</sup>Y. C. Seow, A. Q. Liu, L. K. Chin, X. C. Li, H. J. Huang, T. H. Cheng, and X. Q. Zhou, *Appl. Phys. Lett.* **93**, 084101 (2008).
- <sup>16</sup>K. Campbell, A. Groisman, U. Levy, L. Pangy, S. Mookherjea, D. Psaltis, and Y. Fainman, *Appl. Phys. Lett.* **85**, 6199 (2004).
- <sup>17</sup>D. V. Vezenov, B. T. Mayers, R. S. Conroy, G. M. Whitesides, P. T. Snee, Y. Chan, D. G. Nocera, and M. G. Bawendi, *J. Am. Chem. Soc.* **127**, 8952 (2005).
- <sup>18</sup>X. Cui, L. M. Lee, X. Heng, W. Zhong, P. W. Sternberg, D. Psaltis, and C. Yang, *Proc. Natl. Acad. Sci. U.S.A.* **105**, 10670 (2008).
- <sup>19</sup>M. Hashimoto, B. Mayers, P. Garstecki, and G. M. Whitesides, *Small* **2**, 1292 (2006).
- <sup>20</sup>L. K. Chin, A. Q. Liu, J. B. Zhang, C. S. Lim, and Y. C. Soh, *Appl. Phys. Lett.* **93**, 164107 (2008).
- <sup>21</sup>J. A. Æo Brand Faria, *Microwave Opt. Technol. Lett.* **4**, 224 (1991).
- <sup>22</sup>E. Hecht, *Optics*, 4th ed. (Addison-Wesley, Reading, MA, 2001), p. 476.
- <sup>23</sup>R. B. Thompson, *Fluorescence Sensors and Biosensors* (CRC, Baltimore, 2005).
- <sup>24</sup>N. Damean, S. K. Sia, V. Linder, M. Narovlyansky, and G. M. Whitesides, *Proc. Natl. Acad. Sci. U.S.A.* **102**, 10035 (2005).
- <sup>25</sup>L. Lei, H. Li, J. Shi, and Y. Chen, *Rev. Sci. Instrum.* **81**, 023103 (2010).
- <sup>26</sup>M. R. Bringer, C. J. Gerds, H. Song, J. D. Tice, and R. F. Ismagilov, *Philos. Trans. R. Soc. London, Ser. A* **362**, 1087 (2004).
- <sup>27</sup>H. Song and R. F. Ismagilov, *J. Am. Chem. Soc.* **125**, 14613 (2003).